https://doi.org/10.5194/egusphere-2025-2628
Preprint. Discussion started: 26 June 2025

Impact of stratospheric intrusion on near-surface ozone over the Sichuan Basin in China driven by terrain forcing of Tibetan Plateau

Zhuozhi Shu[a,b], Fumo Yang[c], Guangming Shi[c], Yuqing Zhang[b], Yongjie Huang[a], Xinning Yu[a], Baiwan Pan[a], Tianliang Zhao[b*]

[a] *Chengdu Fluid Dynamics Innovation Center, Chengdu 610031, China*

[b] *Key Laboratory for Aerosol-Cloud-Precipitation of China Meteorological Administration, Collaborative Innovation Center on Forecast and Evaluation of Meteorological Disasters, Nanjing University of Information Science and Technology, Nanjing Jiangsu 210044, China*

[c] *School of Carbon Neutrality Future Technology, National Engineering Research Center on Flue Gas Desulfurization, Sichuan University, Chengdu, 610065, China*

Correspondence: Tianliang Zhao (tlzhao@nuist.edu.cn)

Abstract. Stratospheric ozone (O_3) intrusion acts as a major natural source of tropospheric O_3 affecting atmospheric environment. Targeting a stratospheric intrusion (SI) hotspot, the Tibetan Plateau (TP) with the immediately adjoining O_3 pollution region of Sichuan Basin (SCB) in Southwest China, this study assesses the seasonal contribution of SI to the near-surface O_3 over SCB and reveals the multi-scale coupling mechanisms of atmospheric circulations with the seasonally discrepant terrain effects of the TP. Results show that SI over the TP penetrates deep to the near-surface atmosphere in SCB with a maximum increment of 38.7% in the O_3 level, providing an extra contribution of 11.1–16.0% to regional O_3 pollution. The evolution of South Asian High with the peripheral subsidence in the warm season and the subtropical jet structure in the cold season trigger tropopause folding, driving stratospheric O_3 injecting into the troposphere over the TP. Two primary pathways for SI-derived O_3 entering the near-surface layer over the basin are identified with downslope transport along the TP's leeward slope into the western SCB region and downwind transport to the central and eastern SCB regions associated with the seasonally discrepant effects of TP thermal and mechanical forcing.

Key words: Stratospheric ozone intrusion; Tibetan Plateau's terrain forcing; multi-scale atmospheric circulations; seasonality; Sichuan Basin.

https://doi.org/10.5194/egusphere-2025-2628
Preprint. Discussion started: 26 June 2025

1 Introduction

Ozone (O_3) is a crucial atmospheric chemical composition. Stratospheric ozone (accounting for approximately 90% of the O_3 column) can absorb harmful ultraviolet radiation and protect the surface biosphere, while tropospheric O_3 has emerged as one of the most important air pollutants due to its direct impact on climate change, ecosystem, atmospheric oxidation and human health (Fiore et al., 2002; Feng et al., 2015; Miri et al., 2016). Tropospheric O_3 mainly originates from photochemical production and stratospheric intrusion. The former is characterized by complex nonlinear reactions of O_3 precursors from anthropogenic and natural emissions, involving carbon monoxide, volatile organic compounds and nitrogen oxides, etc. In comparison, the downward transport of stratospheric O_3 not only provides an additional natural source for tropospheric O_3 budgets but causes uncertainties in the near-surface atmospheric environmental changes (Lin et al., 2012; Monk et al., 2015; Liu et al., 2022).

Stratospheric intrusion (SI) is an atmospheric dynamic process occurring between the lower stratosphere and upper troposphere, characterized by the cross-tropopause transport of stratospheric dry airflows into troposphere with rich O_3 and high-level potential vorticity. Multi-scale atmospheric physical processes can trigger SI, including Brewer-Dobson circulation (Brewer, 1949; Dobson et al., 1956; Burchart, 2014), Rossby wave breaking, ENSO, subtropical jet stream, cut-off low, mesoscale convection, and tropopause folding (Waugh and Polvani, 2000; Sprenger et al., 2003; Nieto et al., 2005; Koumoutsaris et al., 2008; Trickl et al., 2011; Neu et al., 2014; Venkat et al., 2016). Approximately 540 ± 140 Tg yr^{-1} stratospheric O_3 enters the troposphere through SI worldwide, contributing ~30% of the tropospheric O_3 column (Stohl et al., 2003; Young et al., 2013). Global SI distribution exhibits a distinct zonal and seasonal asymmetry where the SI hotspots are located in the subtropical regions during late winter and early spring (Škerlak et al., 2014; Williams et al., 2019). The peak of tropopause folding frequency in the period even induces deep SI affecting the lower troposphere (Trickl et al., 2014; Zhao et al., 2021; Chen et al., 2023) which leads to the “exceptional events” on air quality changes (Lin et al., 2015; Pierce and Holloway, 2017). Therefore, cross-layer transport of stratospheric O_3 has a non-negligible potential impact on the near-surface environmental

https://doi.org/10.5194/egusphere-2025-2628
Preprint. Discussion started: 26 June 2025

atmosphere, especially over the susceptive regions of SI (e.g. the west coast of North America, Northwest coast of Africa, eastern Mediterranean and Tibetan Plateau) (Škerlak et al., 2015; Lee et al., 2024).

Tibetan Plateau (TP) is the highest plateau referred as "the roof of the world", located in the mid-latitude region over the Eurasian continent. Large-topography forcing not only modulates hemispheric-scale atmospheric circulation patterns but forms a key window of mass exchange between stratosphere and troposphere (Fu et al., 2006; Li et al., 2018; Huang et al., 2023). As a global hotspot for SI (Škerlak et al., 2014), the impacts of SI on tropospheric O_3 over TP have been extensively studied in recent years. Previous results pointed out that the subtropical jet stream is the principal driving factor for frequent SI events over the TP (Zhang et al., 2010; Luo et al., 2019), dominating the vertical distribution of tropospheric O_3 (Yang et al., 2022; Yin et al., 2023). The O_3-rich airflows from SI can subsequently extend downward to the deep planetary boundary layer by intense turbulent mixing (Chen et al., 2011; Chou et al., 2023), remarkably affecting seasonal and diurnal variations of near-surface O_3 in the region (Ding and Wang, 2006; Ma et al., 2014; Yin et al., 2017). However, with the distinctive topography of TP and frequent SI occurrence, few studies consider the impacts of residual-rich O_3 originating from SI in the free troposphere on atmospheric environmental changes over downstream regions of westerlies, particularly in the typical pollution regions. Addressing this gap, further exploring the impacts of cross-layer O_3 transport from the free troposphere on atmospheric environmental changes in the flat region under the mid-latitude prevailing westerlies is of great value.

Sichuan Basin (SCB), located immediately adjacent to the eastern TP, is recognized as a key region of air pollution complex in China (Lu et al., 2018; Wang et al., 2022) with persistently elevated near-surface O_3 levels (Wei et al., 2022). Regarding the frequent O_3 pollution in SCB, extensive research focuses on the meteorology-emission synergy effects on atmospheric environmental variability, including photochemical regime (Kong et al., 2023), horizontal transport and residual layer mixing (Shu et al., 2023; Wang et al., 2023) and biological source contribution (Xian et al., 2024). Notably, subsidence momentum in the middle and lower free troposphere coexists with the forced uplift of the East Asian monsoon over SCB,

https://doi.org/10.5194/egusphere-2025-2628
Preprint. Discussion started: 26 June 2025

ascribed to mechanical forcing of TP's terrain on prevailing airflows (Xu et al., 2016; Shu et al., 2022), which significantly enhance the vertical interactions of atmospheric pollutants between the free troposphere and atmospheric boundary layer (Shu et al., 2021; Hu et al., 2023). Such regional vertical circulation patterns create excellent atmospheric dynamical conditions for SI to affect the environmental atmosphere over SCB. Therefore, investigating the multi-scale atmospheric circulation coupling mechanisms for stratospheric O_3 into the ambient atmosphere under the plateau-basin topography can provide critical insights into understanding the uncertainty of O_3 pollution in China.

In this study, we aim to quantify the contribution of SI to near-surface O_3 levels over the SCB and then to elucidate the multi-scale circulation coupling mechanisms, in particular focusing on their seasonality with the thermodynamic and dynamical forcing of TP and SCB. The findings of our study are expected to improve the understanding of atmospheric environmental effects of the TP with implications for global and regional environmental changes. Section 2 introduces the observational and reanalysis data, SI episodes selection, WRF-Chem model configuration, experiments design and modeling evaluation results. Section 3 analyzes the temporospatial variations of SIs' impacts on the near-surface layer over the SCB and the terrain-induced atmospheric circulation mechanisms on cross-layer transport of O_3 from stratosphere into the atmospheric boundary layer. Finally, the conclusion are provided in Sect. 4.

2 Data and method

2.1 Observational and reanalysis data

The hourly ground-based observations of environment and meteorology (near-surface O_3 concentrations, 2 m air temperature (T2), 10 m wind speed (WS10) and near-surface relative humidity (RH)) in the study region are respectively obtained from the China National Environmental Monitoring Center (http://www.cnemc.cn/) and the Chinese Meteorological Monitoring Network (http://data.cma.cn/) to evaluate WRF-Chem model performance during the SI episodes.

The hourly 3D meteorological reanalysis data ERA5, with a horizontal resolution of

https://doi.org/10.5194/egusphere-2025-2628
Preprint. Discussion started: 26 June 2025

0.25°×0.25°, are derived from the European Center for Medium-Range Weather Forecasts (https://cds.climate.copernicus.eu/datasets). In the study, this dataset is not only used for SI identification and atmospheric circulation evolution analysis but also serves as the initial and boundary conditions of WRF-Chem experiments. Additionally, the Copernicus Atmosphere Monitoring Service (CAMS) global atmospheric composition reanalysis dataset EAC4 (https://ads.atmosphere.copernicus.eu/datasets) provides 3-hourly chemical species data with a horizontal resolution of 0.75°×0.75° and 60 vertical layers, presenting great credibility in the environment-chemistry field (Inness et al., 2019). The stratospheric O_3 tracer (O_3S) from EAC4 is utilized to verify WRF-Chem simulation applicability for quantifying the transport contributions of SI.

2.2 Selection of seasonal SI episodes

The months of April, July, October and January in 2017 are chosen to characterize seasonal variations in SI and atmospheric circulation patterns in the study as a sequel to our previous studies (Shu et al., 2022; Shu et al., 2023). Corresponding pressure-time cross sections of O_3 averaged over the regions of eastern TP (90–100°E, 28–33°N) and SCB (103–110°E, 28–33°N) are shown in Fig. 1. It is found that frequent stratospheric O_3 intrusions appear over the eastern TP region and significantly affects the middle troposphere with deep SI during April and January but shallow SI in the months of July and October, which is consistent with SI seasonality in the previous results (Škerlak et al., 2014; Luo et al., 2019). With the middle-latitude westerlies transport, the rich O_3 of SI is stretched and deepens into the lower troposphere (reaching 700 hPa layer) over the SCB. In this study, four SI episodes are selected during 12–17 April (EP1), 1–3 July (EP2), 23–28 October (EP3) and 26–30 January (EP4) based on the vertical O_3 structure over the eastern TP and SCB region (Fig.1).

Tropopause folding frequently occurs in the TP characterized by perturbance in dynamical tropopause (2 PVU, potential vorticity unit) isosurface associated with downward cross-tropopause exchange (Sprenger et al., 2003; Luo et al., 2019). As shown in Fig. 2, there exist tropopause folding phenomena that induce O_3-rich stratospheric airflows injecting into the free troposphere between 28–34°N in the study period. Notably, the discrepancy in vertical atmospheric motion seasonality distinguishes the intensity and location of SIs. While

https://doi.org/10.5194/egusphere-2025-2628
Preprint. Discussion started: 26 June 2025

alternating rising and sinking momentum leads to a deep SI event over the central TP during EP1, the deep convection of TP in EP2 triggers strong stratospheric O_3 transport into the lower troposphere (exceeding 160 ppb at 700 hPa layer) over the TP's downstream region SCB. By comparison, a similar vertical structure of SIs in both EP3 and EP4 is featured with the shallow tropopause folding which happens above 300 hPa with weak downward transport of stratospheric O_3.

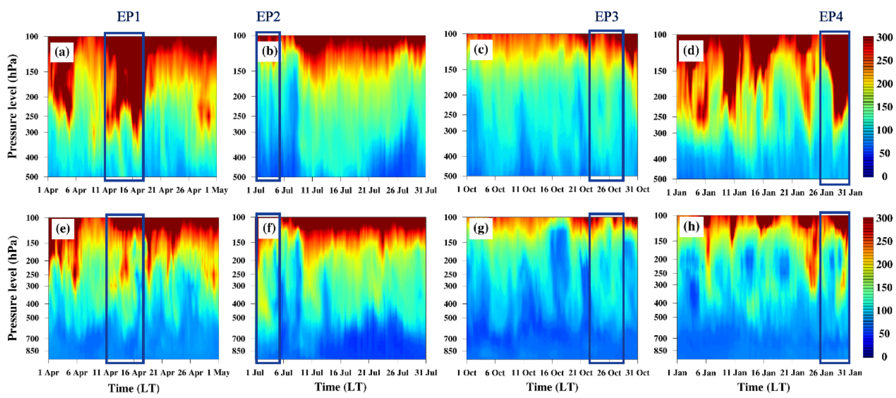

Fig 1. Vertical-time cross sections of O_3 mixing ratio (ppb) over the TP (upper panels) and SCB (lower panels) during April (a,e), July (b,f), October (c,g) and January (d,h) in 2017. The dark-blue boxes respectively represent the selected four SI episodes (EP1–EP4).

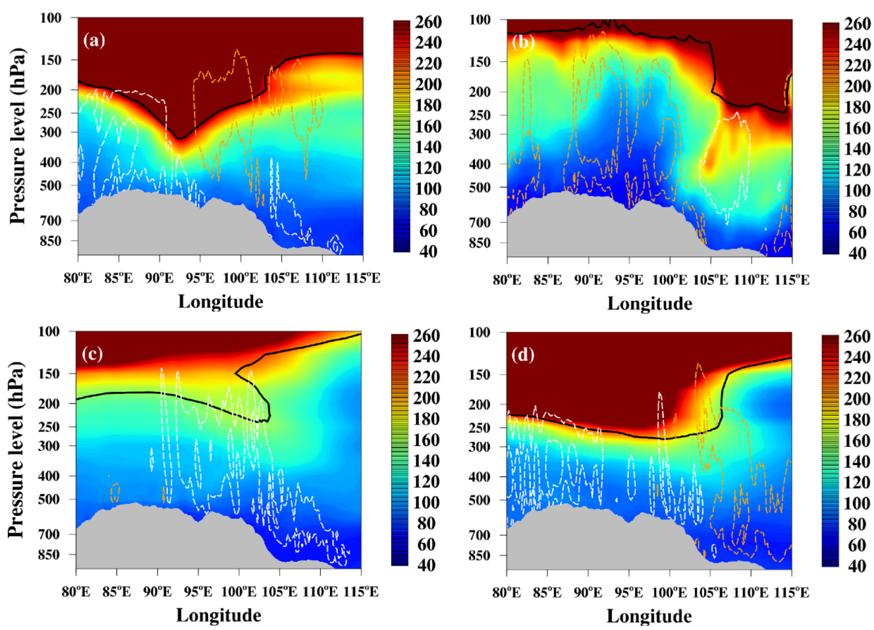

https://doi.org/10.5194/egusphere-2025-2628
Preprint. Discussion started: 26 June 2025

Fig 2. Height-longitude cross sections of O_3 mixing ratio (ppb) averaged between 28–34 °N on (a) 15 April, (b) 1 July, (c) 26 October and (d) 28 January in 2017. The black lines indicate tropopause heights (2 PVU) with the updrafts (brown dashed lines) and downdrafts (white dashed lines) in the region.

2.3 Model configuration and experimental design

The fully online weather-chemistry coupled model WRF-Chem (version 3.8.1) is employed to simulate the variations of meteorology and O_3 for this study. Three nesting domains are constructed (shown in Fig. S1) with horizontal model grid intervals respectively of 48 km, 12 km and 3 km and 40 vertical levels from the surface layer to model top at 50 hPa. The ERA5 reanalysis data are served as the meteorological initial and boundary conditions for WRF-Chem simulation. The first 3 days of simulation are the spin-up time to fully depict SI processes driven by atmospheric circulations. The main physical and chemical schemes are listed in Table S1. Anthropogenic air pollutant emissions are obtained from the Multi-resolution Emission Inventory for China (MEIC, 2017) with a horizontal resolution of 0.25°×0.25° (http://www.meicmodel.org/). And the Model of Emissions of Gases and Aerosols from Nature (MEGAN, v2.1, Guenther et al., 2012) is applied for biogenic emission in WRF-Chem simulation.

The Upper Boundary Condition (UBC) developed by Barth et al. (2012) is incorporated to revise the values of stratospheric atmospheric chemical species ranging from tropopause to 50 hPa due to the lack of stratospheric chemistry in WRF-Chem model. The key chemical species (ie., CH_4, CO, O_3, NO, NO_2, HNO_3, N_2O_5 and N_2O) are fixed to climatological values from global chemistry model results while the tropopause height is calculated by WACCM results (Barth et al., 2012; Lamarque et al., 2012). Zhao et al. (2021) have proved that WRF-Chem can accurately capture the O_3 transport of SI by utilizing UBC scheme. In addition, the integrated process rate (IPR) analysis is used to deepen the understanding of cross-layer O_3 transport mechanism between the free troposphere and atmospheric boundary layer.

Four groups of simulation experiments are conducted to investigate the impact of SI on atmospheric environmental changes over SCB and related plateau-basin terrain forcing effects as follows: 1) Base experiment (Base), utilize UBC scheme to reproduce 3D meteorology and chemistry during the SI episodes; 2) stratospheric O_3 sensitivity experiment (EXP_{stro3}), other

https://doi.org/10.5194/egusphere-2025-2628
Preprint. Discussion started: 26 June 2025

settings are identical to Base but discard UBC scheme and default O_3 values (set as zero) above tropopause in WRF-Chem simulation; 3) the basin-terrain sensitivity experiment (EXP_{terr}), basin-filling terrain replace the default deep-basin terrain height (take Base as a benchmark), which refers to a zonal linear interpolation method (Zhang et al., 2019), but remain surface static fields (e.g. landuse and soil types) unchanged; 4) both stratospheric O_3 and basin-terrain sensitivity experiment ($EXP_{stro3+terr}$), run with basin-filling terrain compared with EXP_{stro3}. The difference between Base and EXP_{stro3} ($\triangle x$ = Base – EXP_{stro3}, including O_3, horizontal transport (ADVH) and vertical transport (ADVZ)) is denoted by the quantitative contribution of SI, and $\triangle O_3$basin = EXP_{terr} – $EXP_{stro3+terr}$ is used to investigate the deep-basin terrain forcing mechanism on cross-layer transport of O_3 during the SI episodes.

2.4 Modeling evaluation

Our model results can reasonably reproduce the variations in meteorology both at the near-surface layer and within atmospheric boundary layer by comparing simulated and observed results during the four representative months of April, July, October and January in 2017 (Shu et al., 2023). The statistical metrics of T2, WS10 and RH are also listed in Table S2, which meets the model criteria for applications recommended by Emery et al. (2001).

Regarding the accuracy of simulated surface O_3 concentrations, WRF-Chem simulation results also show a good agreement with ground-based environmental observation at 18 urban sites in the SCB (Shu et al., 2023). Fig. S2 shows the comparisons of near-surface O_3 variations between simulation and observation at two representative megacities of Chengdu and Chongqing during the SI episodes, respectively with the index of agreement (IOA) of 0.68–0.91 (Chengdu) and 0.56–0.89 (Chongqing) and mean fractional error (MFE) ranged of 10.8–20.8% and 18.9–29.7%. Whereafter, the spatial distribution of near-surface $\triangle O_3$ is compared with O_3S of EAC4 reanalysis data. As shown in Fig. S3, though there exists an overestimation in EP4, modeling results properly present the impacts of SI on near-surface O_3 levels in our study region. Overall, the evaluation results above present good modeling reliability for the following analyses.

https://doi.org/10.5194/egusphere-2025-2628
Preprint. Discussion started: 26 June 2025

3 Results and Discussion

3.1 Impacts of SI on near-surface O_3 levels over the SCB

To illustrate the impacts of SIs on atmospheric environmental changes, the temporospatial variations of $\triangle O_3$ at the near-surface layer are analyzed in SCB and surrounding regions based on the WRF-Chem experiments results of the innest domain. The environmental atmosphere of high-elevation regions is significantly influenced by O_3-rich stratosphere airflows when SI episode happens (Bracci et al., 2021; Yin et al., 2017). A similar spatial distribution pattern of $\triangle O_3$ presents that SI aggravates O_3 levels in the near-surface environmental atmosphere over Southwest China with higher O_3 enhancements (exceeding 16 ppb) in the eastern TP rather than lower levels (approximately ~10 ppb) over the SCB in all episodes (Fig. 3). Obviously, these results show the plateau-basin topography effects on $\triangle O_3$ distribution over the region, and even confirm the connection between air quality changes in the adjoining polluted region of SCB and SI episodes occurring over the TP and surrounding area. Aiming to the SCB region, SI-induced near-surface O_3 increments exhibit higher values during EP1 in springtime and lower in EP4 of wintertime with a significant extension gradient of $\triangle O_3$ levels at the western boundary. The phenomena involve downward O_3 transport for SI from TP to SCB with prevailing westerlies under the distinctive terrain forcing, which will be further investigated in Sect. 3.2.

To assess the impacts of SI transport on atmospheric environmental changes over the SCB, we calculate the hourly concentrations of $\triangle O_3$ and its relative contribution rate to near-surface O_3 levels averaged over the SCB region. As shown in Fig. 4, stratospheric O_3 transport affects SCB mainly starting on 13 April, 1 July, 26 October and 29 January, respectively, with $\triangle O_3$ averages of 6.3 ppb, 5.5 ppb, 4.3 ppb and 3.1 ppb, contributing 18.2%, 15.4%, 12.7% and 17.0% of total concentrations for near-surface O_3 in our study period. It should be pointed out that there exist two SI episodes happened in the TP during our study period of EP1 respectively on 11 April and 15 April (Fig. 1), leading to persistent $\triangle O_3$ transport contribution for SI during 13–18 April over the SCB. A diurnal fluctuation appears in the SI episodes with higher $\triangle O_3$ levels in the daytime and lower those during the nighttime, reflecting the impacts of vertical mixing within atmospheric boundary layer on downward O_3 transport. It should be noteworthy

https://doi.org/10.5194/egusphere-2025-2628
Preprint. Discussion started: 26 June 2025

that the SCB is experiencing regional O_3 pollution on both 14–15 April and 1–2 July in 2017 during the SI episodes periods (Fig. S4), in which daily maximum 8-hour average O_3 concentrations exceed 160 μg m^{-3}. The contribution of SI transport induces O_3 pollution aggravation in the SCB with an extra contribution approximately of 11.1–16.0%. It highlights the non-negligible role of SI in regional air quality changes over the polluted region SCB, and thereby deserves more concern for the prevention and control of air pollution in the region.

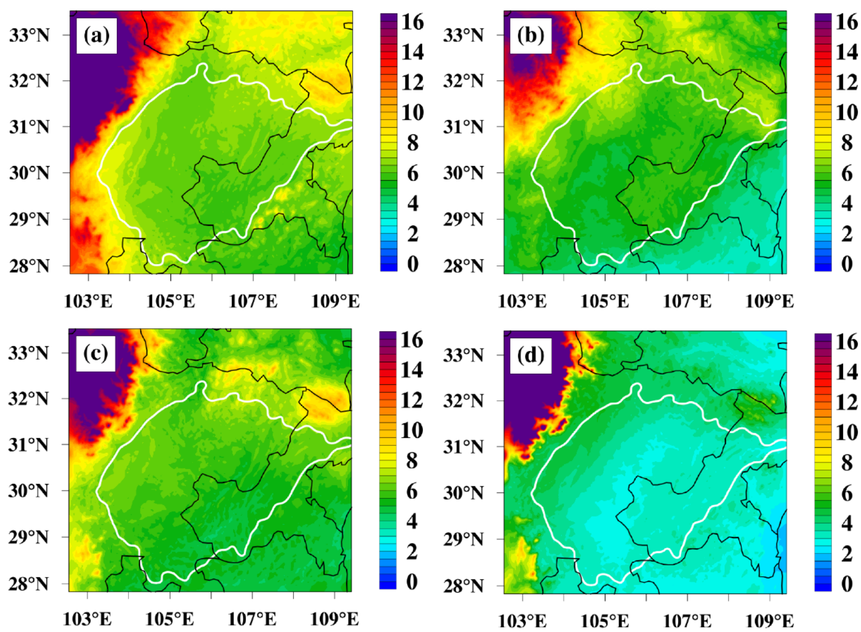

Fig 3. Spatial distribution of near-surface $\triangle O_3$ (ppb, color contours) during SI events (a) EP1, (b) EP2, (c) EP3 and (d) EP4. The thick white lines roughly outline the SCB region.

https://doi.org/10.5194/egusphere-2025-2628
Preprint. Discussion started: 26 June 2025

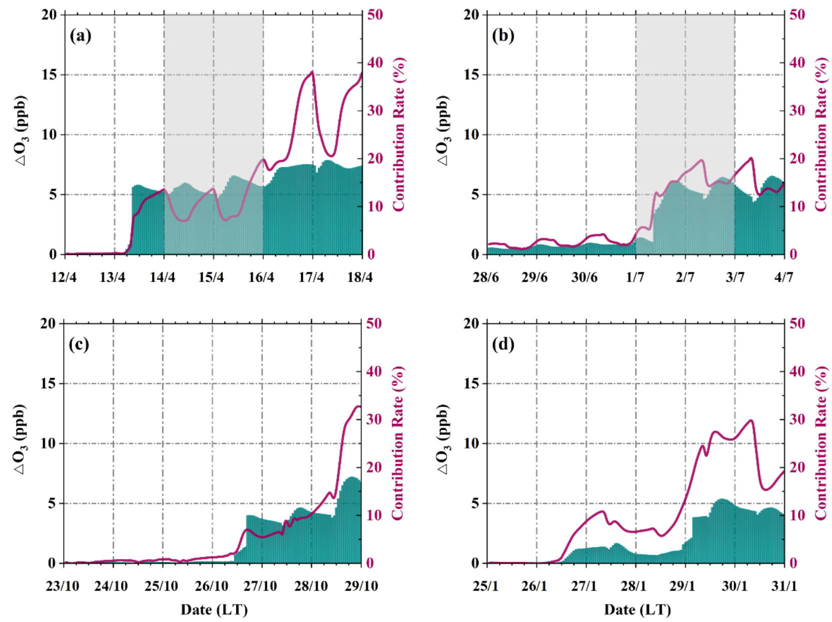

Fig 4. Hourly variations of near-surface $\triangle O_3$ (ppb, blue-filled areas) during the period of SI events (a) EP1, (b) EP2, (c) EP3 and (d) EP4 with its relative contribution proportions to the environmental atmosphere (dark red curve) averaged over the SCB. The gray shade indicates the regional O_3 pollution period.

3.2 Terrain-forced atmospheric circulations driving downward transport of stratospheric O_3

Now that the impacts of SI on near-surface O_3 levels over the SCB have been estimated above, we further address the question of how atmospheric circulations persistently drive airflows descent process across tropopause and atmospheric boundary layer simultaneously. In particular, the seasonal variations in large-topography thermodynamic and mechanical forcing of TP and SCB affect multi-scale atmospheric circulation coupling, establishing unique transport pathways from the stratosphere to near-surface atmosphere of SCB in common.

3.2.1 Mechanisms of SI occurrence

Seasonal variations in atmospheric circulation patterns at 200 hPa are investigated during the SIs' initial phase (Fig. 5). The results indicate that SI occurrence in the TP and surrounding regions is strongly related to the South Asian High (SAH) and subtropical jet stream activity.

https://doi.org/10.5194/egusphere-2025-2628
Preprint. Discussion started: 26 June 2025

In the summer monsoon period (EP1 and EP2), intense sensible heating over the elevated topography of Iranian plateau and TP induces deep convection extending to the lower stratosphere. A pronounced anticyclone circulation is formed at 200 hPa over the Northern Hemisphere. SAH triggers deep SI events and transports high-latitude O_3-rich air intruding into the lower troposphere by strengthening zonal airflow intersection (Wang et al., 2020; Zhang et al., 2022). As shown in Fig. 5, Iranian High, one part of the SAH, exhibits an anticyclonic circulation on the western side of TP during EP1, while the summertime TP's dynamical pumping (Fig. 1) reinforces SAH evolution controlling TP region (with an intensity of 12,300 gpm). Coupled with the prevailing southwesterly monsoon, a cut-off trough is respectively produced over the central TP (EP1) and downstream regions (EP2). Correspondingly, strong atmospheric downdraft motion drives stratospheric air into the free troposphere with an abnormally high-level belt of potential vorticity (of ~8 PVU and ~6 PVU) over the region.

In addition, the subtropical westerly jet is also an important dynamical driving factor that induces tropopause folding with SI over the TP. Attributed to TP's location in the mid-latitude region, southward movement of subtropical westerly jet prevails over the TP in the wintertime, which intensifies tropopause disturbance (Sprenger et al., 2003), leading to frequent SI occurrence over the TP and its surrounding regions (Chen et al., 2011). Westerlies are gradually strengthened over the TP region controlled by subtropical jet from EP3 to EP4, forming a significant banded structure of tropopause folding in the mid-latitude region, which is represented by a high-value region of potential vorticity at 200 hPa approximately with 4–7 PVU. These results reveal the SI triggering mechanisms under seasonal typical atmospheric circulation patterns over hotspot region TP to a certain extent. It is worth noting that the anomalously high levels of potential vorticity appear in most regions over 40 °N, which is ascribed to the combination of zonal distribution of atmospheric tropopause heights and seasonal subtropical westerly jet stream shifts.

https://doi.org/10.5194/egusphere-2025-2628
Preprint. Discussion started: 26 June 2025

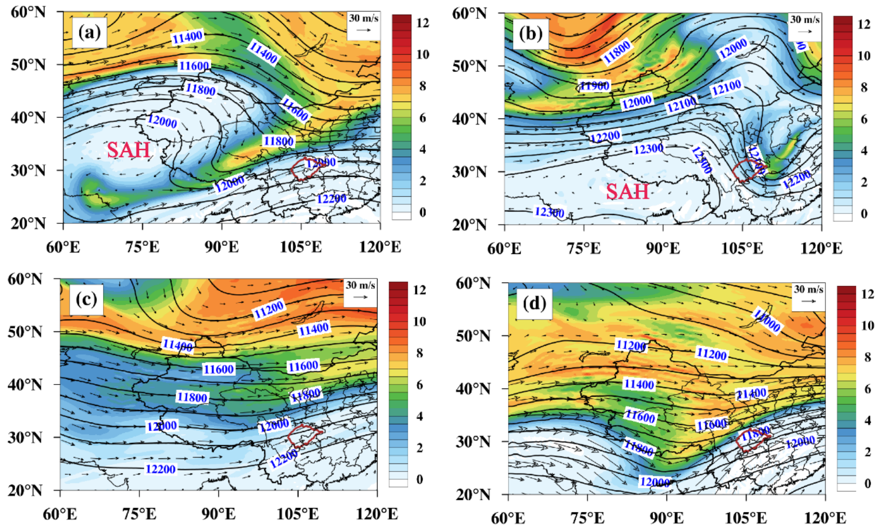

Fig 5. Spatial distribution of geopotential height (in gpm; black lines), wind vectors and potential vorticity (units in PVU, 10^{-6} m^2 s^{-1} K kg^{-1}; color shaded) at 200 hPa during (a) 15 April, (b) 1 July, (c) 26 October and (d) 28 January in 2017. The SAH indicates the South Asian High in the upper troposphere.

3.2.2 Stratospheric O_3 transport from free troposphere to near-surface atmosphere

Accompanied by high-level O_3 of SI entering the middle troposphere, the subsidence momentum at the eastern slope of TP keeps downward transport into the lower troposphere over the SCB. Fig. 6 shows that a similar atmospheric circulation pattern is manifested at 500 hPa during SI episodes with propagation of ridge and trough from the upper troposphere (Fig. 5). In EP1 and EP2, deepened geopotential ridges steer high-latitude cold air southward intrusion with intense subsidence in the middle-level troposphere of SCB. Whereas during the periods of EP3 and EP4 episodes, relatively straight free-troposphere westerlies are forcedly elevated at the windward slope of western TP region, while sinking airflows occur at the leeside slope of plateau over the eastern TP and downstream SCB due to the mechanical forcing of TP's large topography. That is, although there is a significant seasonal discrepancy in atmospheric circulation in the middle and upper troposphere, rich O_3 originating from SI is inevitably injected into the lower troposphere over SCB through the coupling effects of atmospheric vertical movements under the distinctive terrain forcing of TP.

https://doi.org/10.5194/egusphere-2025-2628
Preprint. Discussion started: 26 June 2025

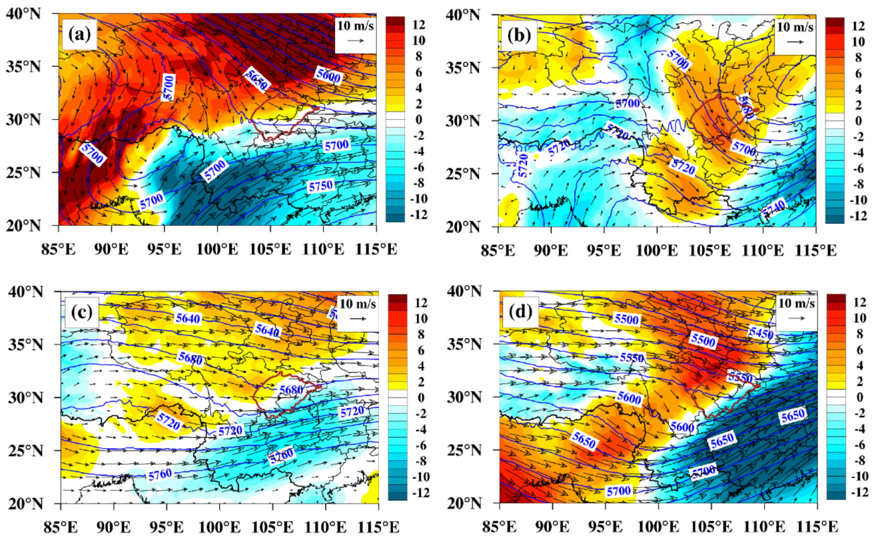

Fig 6. Geopotential height (in gpm; blue contours), wind vectors and vertical velocity (pa s^{-1}; color shaded) at 500 hPa on (a) 16 April, (b) 1 July, (c) 26 October and (d) 29 January 2017.

The regional atmospheric structure over SCB is strongly subject to downdraft at TP's leeside slope (Xu et al., 2016, Shu et al., 2022), where vertical circulation configuration is characterized by the free-troposphere downdraft westerlies and easterly Asian monsoon within the atmospheric boundary layer, constructing a large-scale vertical wind shear and vertical vortices (Ning et al., 2019; Shu et al., 2021). The interaction of regional circulations is conducive to cross-layer exchanges of air pollutants over the SCB (Shu et al., 2023).

Fig.7 shows the lower-troposphere vertical circulation patterns with their impacts on the downward transport of SI to the near-surface layer in SCB. Subsidence momentum dominates the SCB region driving high levels of O_3 in the middle troposphere to expand into the near-surface atmosphere, with a remarkable vertical $\triangle O_3$ gradient approximately of 20 ppb. There are two primary pathways affecting air quality in the SCB for SI O_3-rich airflows. One branch is delivered along the downslope of the plateau-basin transition zone into the western SCB, thermally driven by mountain-plains solenoid between the plateau and flat SCB regions. It is a quasi-horizontal transport process within the atmospheric boundary layer from the high-altitude eastern TP to western SCB, which results in a horizontal gradient of $\triangle O_3$ expansion to the west of SCB (Fig. 3). The other pathway is directly downwind injection of $\triangle O_3$ from the free

https://doi.org/10.5194/egusphere-2025-2628
Preprint. Discussion started: 26 June 2025

troposphere into atmospheric boundary layer, which is related to entrainment at the top of boundary layer (Škerlak et al., 2019), mainly over the central and eastern regions of SCB. IPR analysis also verifies the results that horizontal transport dominates $\triangle O_3$ changes over the plateau-basin transition region of western SCB, but vertical transport induces the increments of near-surface O_3 levels over the central and eastern flat region of SCB during SI episodes (shown in Fig. 7). Another notable feature is Asian Monsoon circulation with intensified easterly wind vectors over the SCB in both EP2 and EP4, facilitating cross-layer transport of SI O_3 by formed vertical vortex in EP2 and EP4, respectively below the heights of 3 km and 2 km (a.s.l.). It reflects the modulation of plateau-basin topography on the free troposphere-atmospheric boundary layer O_3 transport of SI over SCB.

https://doi.org/10.5194/egusphere-2025-2628
Preprint. Discussion started: 26 June 2025

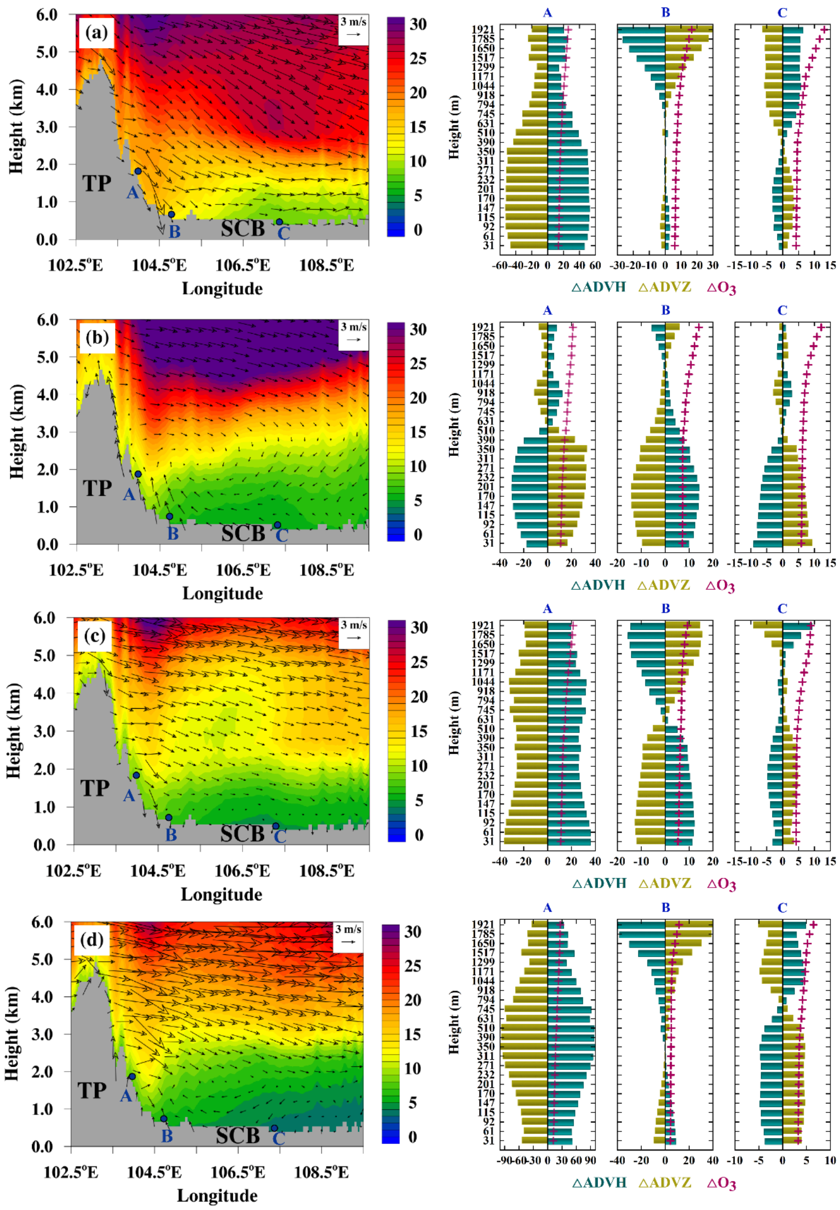

Fig 7. Height-longitude cross-sections of $\triangle O_3$ (ppb, color contours) and wind vectors averaged between 28–33°N on (a) 16 April, (b) 1 July, (c) 26 October and (d) 29 January 2017 (left panel) with correspondingly IPR on horizontal transport (△ADVH) and vertical transport (△ADVZ) respectively at points A (plateau region), B (western edge of SCB) and C (central SCB).

https://doi.org/10.5194/egusphere-2025-2628
Preprint. Discussion started: 26 June 2025

3.2.3 Discussion on SI-induced environmental atmosphere changes

Additionally, △O_3basin in the lower troposphere is also analyzed to further investigate the modulation effect of deep-basin terrain structure on cross-layer O_3 transport between the free troposphere and near-surface environmental atmosphere during SI episodes. We found that the low-lying basin topography of SCB mitigates regional O_3 pollution deterioration derived from SIs. As shown in Fig. S5 in the Supplementary information, westerlies straightly penetrate the regional atmospheric boundary layer of SCB region with stronger quasi-horizontal transboundary transport of TP's rich stratospheric O_3. It would aggravate SI-induced O_3 enhancements over the SCB's environmental atmosphere, with averages of 9.1 ppb (EP1), 7.8 ppb (EP2), 6.6 ppb (EP3) and 8.0 ppb (EP4), respectively corresponding to the increments of 44.4 %, 41.8 %, 53.5 % and 158.1 % compared to real deep-basin topography. These results illustrate that TP modulates stratospheric O_3 transport between the free troposphere and environmental atmosphere while the deep-basin structure of SCB varies O_3 transport patterns over the region, revealing an essential terrain-forced mechanism of large plateau-basin topography on cross-layer SI transport.

4 Conclusion

Aiming at the global SI hotspot TP (Škerlak et al., 2014) and adjoining typical polluted SCB regions, multiple-source meteorology-environment observational and reanalysis data coupled with WRF-Chem simulations are employed to quantify the impacts of stratospheric O_3 intrusion on the near-surface environmental atmosphere over SCB in the study. Four SI episodes are targeted to investigate multi-scale atmospheric circulation coupling mechanisms and their seasonality on cross-layer transport of stratospheric O_3 under distinctive plateau-basin terrain forcing. Results can deepen the understanding of regional O_3 pollution genesis with the exceptional natural sources contribution derived from the stratosphere.

The occurrence of SI in the TP and surrounding regions exerts a non-negligible impact on aggravating near-surface O_3 levels over the downstream SCB, which is primarily characterized by the horizontal expansion of SI-derived O_3 levels from the west edge of SCB to central region. Such downward O_3 transport contributes an average increase of ~8.0 ppb, contributing ~38.7%

https://doi.org/10.5194/egusphere-2025-2628
Preprint. Discussion started: 26 June 2025

of environmental changes in the SCB. Larger SI-induced near-surface O_3 increments appear during EP1 and EP2 episodes respectively in April and July, providing an extra contribution of 11.1–16.0 % to regional O_3 pollution formation over the SCB. The results reveal the cross-layer O_3 transport affecting air quality from stratosphere to the free troposphere and ultimately into atmospheric boundary layer.

Whereafter, we explore seasonal terrain-forcing atmospheric circulation coupling mechanisms on cross-layer O_3 transport. Fig. 8 summarizes the primary triggering effects as follows: The unique plateau's thermodynamic forcing in warm seasons but mechanical forcing in the cold season respectively modulates stratospheric O_3-rich air injection into the near-surface atmosphere over the SCB affecting regional air quality. On one hand, the joint thermal forcing of TP and Iranian Plateau in EP1 and EP2 triggers stratospheric O_3 intrusion over the TP and surrounding regions by peripheral subsidence of South Asian High in the upper troposphere. Stratospheric O_3 is steered by intensified zonal interaction of westerlies driving high-latitude cold airflows downward transport into the adjacent SCB region. On the other hand, the southward retreat of subtropical jet stream during the EP3 and EP4 leads to SIs occurrence over the TP. With the TP's mechanical forcing on stronger middle-troposphere westerlies, leeward slope subsidence deliver high-level stratospheric O_3 to the lower troposphere over the SCB region. Two primary pathways are identified to affect air quality over the SCB for SI-derived O_3, involving along the TP's downslope into the western SCB and directly downwind transport into atmospheric boundary layer over the central and eastern regions of SCB. The existence of low-lying deep basin structure weakens the contribution of SI to regional environmental atmosphere in the SCB.

This modeling study investigats the four episodes for a seasonal assessment of the contribution of stratospheric O_3 intrusion to the SCB regions in Southwest China, highlighting the multi-scale atmospheric circulation coupling mechanisms under the distinctive plateau-basin terrain forcing. In the future, it is necessary to generalize the climatology of SI impacts on near-surface environmental atmosphere in the region with multi-year observation and simulation.

https://doi.org/10.5194/egusphere-2025-2628
Preprint. Discussion started: 26 June 2025

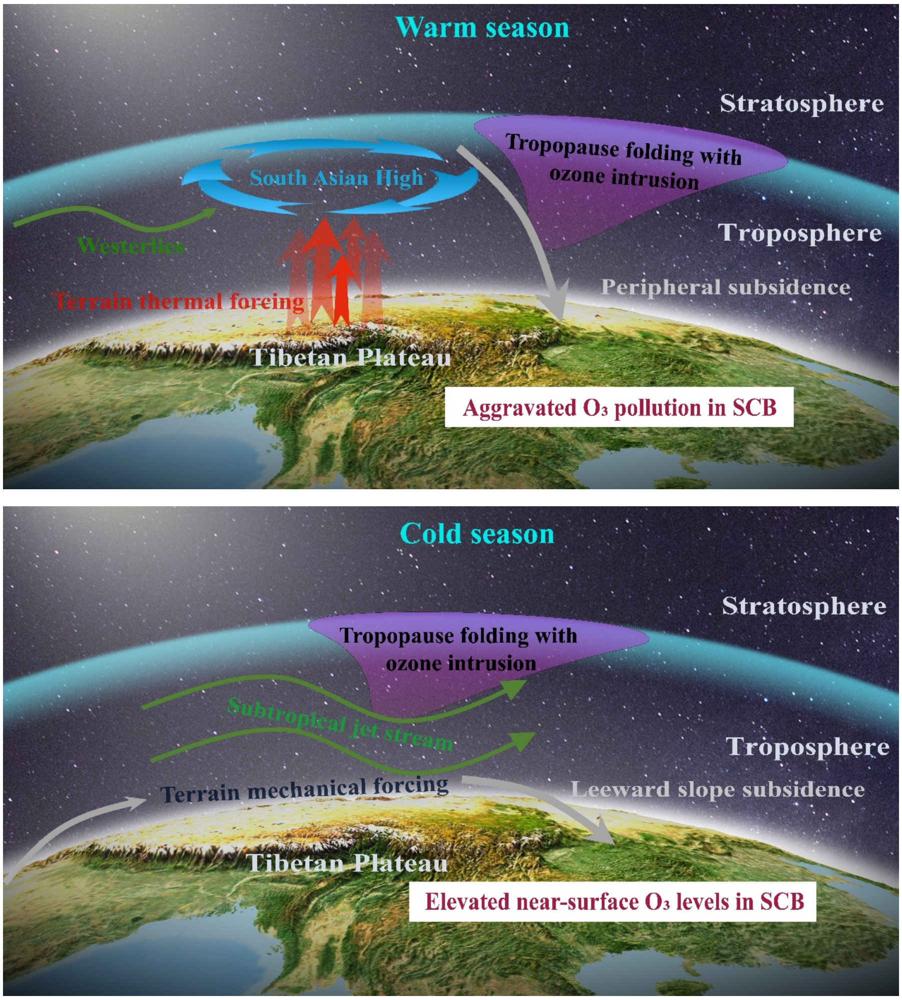

Fig 8. Diagram on the cross-layer transport of stratospheric O_3 on regional atmospheric environmental changes over SCB driven by mult-scale atmospheric circulation pattern with the seasonally discrepant terrain effects of TP.

Data availability

The ground-based environment and meteorology data are respectively available at the China National Environmental Monitoring Center (http://www.cnemc.cn/) and the Chinese Meteorological Monitoring Network (http://data.cma.cn/). ERA5 data are derived from Copernicus Climate Change Service (C3S) Climate Date Store (https://cds.climate.copernicus.eu/datasets). EAC4 reanalysis data are obtained from Copernicus Atmosphere Monitoring Service (https://ads.atmosphere.copernicus.eu/datasets).

All data used in this paper can be provided upon request from Zhuozhi Shu (shuzhuozhi@foxmail.com).

Author Contributions

Conceptualization: ZS, TZ, FY, GS, YZ. Investigation: ZS, YH, XY, BP. Methodology: ZS, TZ, YZ. Validation: YH, XY, BP. Writing (original draft preparation): ZS, TZ, YZ. Writing (review and editing): ZS, TZ, YZ, FY, GS. All of the authors provided commentary on the paper.

Competing interest

The authors declare that they have no conflict of interest.

Acknowledgments

This work was supported jointly by the National Natural Science Foundation of China (Grant No. 42405195 and 42275196), the National Key Research and Development Program of China (Grant No. 2022YFC3701204 and 2023YFC3709301) and the National Natural Science Foundation of China (Grant No. 42207134 and 42465008).

References

Barth, M. C., Lee, J., Hodzic, A., Pfister, G., Skamarock, W. C., Worden, J., Wong, J., and Noone, D.: Thunderstorms and upper troposphere chemistry during the early stages of the 2006 North American Monsoon. Atmospheric Chemistry and Physics, 12, 11003–11026. https://doi.org/10.5194/acp-12-11003-2012, 2012.

Bracci, A., Cristofanelli, P., Sprenger, M., Bonafè, U., Calzolari, F., Duchi, R., Laj, P., Marinoni, A., Roccato, F., Vuillermoz, E., and Bonasoni, P.: Transport of Stratospheric Air Masses to the Nepal Climate Observatory–Pyramid (Himalaya; 5079 m MSL): A Synoptic-Scale Investigation. Journal of Applied Meteorology and Climatology, 51, 1489–1507. https://doi.org/10.1175/JAMC-D-11-0154.1, 2012.

Brewer, A.W.: Evidence for a world circulation provided by the measurements of helium and water vapour distribution in the stratosphere. Quarterly Journal of the Royal Meteorological Society, 75, 351–363. https://doi.org/10.1002/qj.49707532603, 1949.

Butchart, N.: The Brewer-Dobson circulation. Reviews of Geophysics, 52, 157–184. https://doi.org/10.1002/2013RG000448, 2014.

Chen, X., Ma, Y., Kelder, H., Su, Z., and Yang, K.: On the behaviour of the tropopause folding events over the Tibetan Plateau. Atmospheric Chemistry and Physics, 11, 5113–5122. https://doi.org/10.5194/acp-11-5113-2011, 2011.

Chen, Z., Liu, J., Cheng, X., Yang, M., and Shu, L.: Stratospheric influences on surface ozone increase during the COVID-19 lockdown over northern China. npj Climate and Atmospheric Science, 6, 76. https://doi.org/10.1038/s41612-023-00406-2, 2023.

Chou, Y., Huang, Q., Zhang, Yongpeng, Luo, J., Wang, M., Liao, H., Zhang, Y., and Bai, Z.: Impacts of deep boundary layer on near-surface ozone concentration over the Tibetan Plateau. Atmospheric

https://doi.org/10.5194/egusphere-2025-2628
Preprint. Discussion started: 26 June 2025

Environment, 294, 119532. https://doi.org/10.1016/j.atmosenv.2022.119532, 2023.

Ding, A., and Wang, T.: Influence of stratosphere-to-troposphere exchange on the seasonal cycle of surface ozone at Mount Waliguan in western China. Geophysical Research Letters, 33, L03803. https://doi.org/10.1029/2005GL024760, 2006.

Dobson, G. M. B.: Origin and distribution of the polyatomic molecules in the atmosphere. Proceedings Royal Society Lond. A, 236, 187–193. https://doi.org/10.1098/rspa.1956.0127, 1956.

Duan, A., and Wu, G.: Weakening Trend in the Atmospheric Heat Source over the Tibetan Plateau during Recent Decades. Part I: Observations. Journal of Climate, 21, 3149–3164. https://doi.org/10.1175/2007JCLI1912.1, 2008.

Emery, C.A., Tai, E., and Yarwood, G.: Enhanced Meteorological Modeling and Performance Evaluation for Two Texas Ozone Episodes. Prepared for the Texas Natural Resource Conservation Commission, by Environ International Corp. https://api.semanticscholar.org/CorpusID:127579774, 2001.

Feng, Z., Hu, E., Wang, X., Jiang, L., and Liu, X.: Ground-level O_3 pollution and its impacts on food crops in China: A review. Environmental Pollution, 199, 42–48. https://doi.org/10.1016/j.envpol.2015.01.016, 2015.

Fiore, A. M., Jacob, D. J., Field, B. D., Streets, D. G., Fernandes, S. D., and Jang, C.: Linking ozone pollution and climate change: The case for controlling methane. Geophysical Research Letter,s 29, 25-1-25–4. https://doi.org/10.1029/2002GL015601, 2002.

Fu, R., Hu, Y., Wright, J. S., Jiang, J. H., Dickinson, R. E., Chen, M., Filipiak, M., Read, W. G., Waters, J. W., and Wu, D. L.: Short circuit of water vapor and polluted air to the global stratosphere by convective transport over the Tibetan Plateau. Proceedings of the National Academy of Sciences, 103, 5664–5669. https://doi.org/10.1073/pnas.0601584103, 2006.

Guenther, A. B., Jiang, X. and Heald, C. L., Sakulyanontvittaya, T., Duhl, T., Emmons, L. K., and Wang, X. The Model of Emissions of Gases and Aerosols from Nature version 2.1 (MEGAN2.1): an extended and updated framework for modeling biogenic emissions. Geoscientific Model Development, 5, 1471–1492. https://doi.org/10.5194/gmd-5-1471-2012, 2012.

Hu, J., Zhao, T., Liu, J., Cao, L., Wang, C., Li, Y., Shi, C., Tan, C., Sun, X., Shu, Z., and Li, J.: Exploring the ozone pollution over the western Sichuan Basin, Southwest China: The impact of diurnal change in mountain-plains solenoid. Science of the Total Environment, 839, 156264. https://doi.org/10.1016/j.scitotenv.2022.156264, 2022.

Huang, J., Zhou, X., Wu, G., Xu, X., Zhao, Q., Liu, Yimin, Duan, A., Xie, Y., Ma, Y., Zhao, P., Yang, S., Yang, K., Yang, H., Bian, J., Fu, Y., Ge, J., Liu, Yuzhi, Wu, Q., Yu, H., and Qie, K.: Global Climate Impacts of Land-Surface and Atmospheric Processes Over the Tibetan Plateau. Reviews of Geophysics, 61. https://doi.org/10.1029/2022RG000771, 2023.

Inness, A., Ades, M., Agustí-Panareda, A., Barré, J., Benedictow, A., Blechschmidt, A.-M., Dominguez, J.J., Engelen, R., Eskes, H., Flemming, J., Huijnen, V., Jones, L., Kipling, Z., Massart, S., Parrington, M., Peuch, V.-H., Razinger, M., Remy, S., Schulz, M., and Suttie, M.: The CAMS reanalysis of atmospheric composition. Atmospheric Chemistry and Physics, 19, 3515–3556. https://doi.org/10.5194/acp-19-3515-2019, 2019.

Kong, L., Zhou, L., Chen, D., Luo, L., Xiao, K., Chen, Y., Liu, H., Tan, Q., and Yang, F.: Atmospheric oxidation capacity and secondary pollutant formation potentials based on photochemical loss of VOCs in a megacity of the Sichuan Basin, China. Science of the Total Environment, 901, 166259. https://doi.org/10.1016/j.scitotenv.2023.166259, 2023.

Koumoutsaris, S., Bey, I., Generoso, S., and Thouret, V.: Influence of El Niño–Southern Oscillation on

https://doi.org/10.5194/egusphere-2025-2628
Preprint. Discussion started: 26 June 2025

the interannual variability of tropospheric ozone in the northern midlatitudes. Journal of Geophysical Research: Atmospheres, 113. https://doi.org/10.1029/2007JD009753, 2008.

Lamarque, J. -F., Emmons, L. K., Hess, P. G., Kinnison, D. E., Tilmes, S., Vitt, F., Heald, C. L., Holland, E. A., Lauritzen, P. H., Neu, J., Orlando, J. J., Rasch, P. J., and Tyndall, G. K.: CAM-chem: description and evaluation of interactive atmospheric chemistry in the Community Earth System Model. Geoscientific Model Development, 5, 369–411. https://doi.org/10.5194/gmd-5-369-2012, 2012.

Lee, J., Wu, Y., and Wang, X.: The evolutions and large-scale mechanisms of summer stratospheric ozone intrusion across global hotspots. Journal of Geophysical Research: Atmospheres, 129(4), e2023JD039877. https://doi.org/10.1029/2023JD039877, 2024.

Li, D., Vogel, B., Müller, R., Bian, J., Günther, G., Li, Q., Zhang, J., Bai, Z., Vömel, H., and Riese, M.: High tropospheric ozone in Lhasa within the Asian summer monsoon anticyclone in 2013: influence of convective transport and stratospheric intrusions. Atmospheric Chemistry and Physics, 18, 17979–17994. https://doi.org/10.5194/acp-18-17979-2018, 2018.

Lin, M., Fiore, A. M., Cooper, O. R., Horowitz, L. W., Langford, A. O., Levy II, H., Johnson, B. J., Naik, V., Oltmans, S. J., and Senff, C. J.: Springtime high surface ozone events over the western United States: Quantifying the role of stratospheric intrusions. Journal of Geophysical Research: Atmospheres, 117. https://doi.org/10.1029/2012JD018151, 2012.

Lin, M., Fiore, A. M., Horowitz, L. W., Langford, A. O., Oltmans, S. J., Tarasick, D., and Rieder, H. E.: Climate variability modulates western US ozone air quality in spring via deep stratospheric intrusions. Nature Communications, 6, 7105. https://doi.org/10.1038/ncomms8105, 2015.

Liu, J., Strode, S. A., Liang, Q., Oman, L. D., Colarco, P. R., Fleming, E. L., Manyin, M. E., Douglass, A. R., Ziemke, J. R., Lamsal, L. N., and Li, C.: Change in Tropospheric Ozone in the Recent Decades and Its Contribution to Global Total Ozone. Journal of Geophysical Research: Atmospheres, 127, e2022JD037170. https://doi.org/10.1029/2022JD037170, 2022.

Lu, X., Hong, J., Zhang, L., Cooper, O. R., Schultz, M. G., Xu, X., Wang, T., Gao, M., Zhao, Y., and Zhang, Y.: Severe Surface Ozone Pollution in China: A Global Perspective. Environmental Science & Technology Letters, 5, 487–494. https://doi.org/10.1021/acs.estlett.8b00366, 2018.

Luo, J., Liang, W., Xu, P., Xue, H., Zhang, M., Shang, L., and Tian, H.: Seasonal Features and a Case Study of Tropopause Folds over the Tibetan Plateau. Advances in Meteorology, 2019, 1–12. https://doi.org/10.1155/2019/4375123, 2019.

Ma, J., Lin, W. L., Zheng, X., Xu, X., Li, Z., and Yang, L.: Influence of air mass downward transport on the variability of surface ozone at Xianggelila Regional Atmosphere Background Station, southwest China. Atmospheric Chemistry and Physics, 14, 5311–5325. https://doi.org/10.5194/acp-14-5311-2014, 2014.

Miri, M., Derakhshan, Z., Allahabadi, A., Ahmadi, E., Oliveri Conti, G., Ferrante, M., and Aval, H. E.: Mortality and morbidity due to exposure to outdoor air pollution in Mashhad metropolis, Iran. The AirQ model approach. Environmental Research, 151, 451–457. https://doi.org/10.1016/j.envres.2016.07.039, 2016.

Monks, P. S., Archibald, A. T., Colette, A., Cooper, O., Coyle, M., Derwent, R., Fowler, D., Granier, C., Law, K. S., Mills, G. E., Stevenson, D. S., Tarasova, O., Thouret, V., von Schneidemesser, E., Sommariva, R., Wild, O., and Williams, M.L.: Tropospheric ozone and its precursors from the urban to the global scale from air quality to short-lived climate forcer. Atmospheric Chemistry and Physics, 15, 8889–8973. https://doi.org/10.5194/acp-15-8889-2015, 2015.

Neu, J. L., Flury, T., Manney, G. L., Santee, M. L., Livesey, N. J., and Worden, J.: Tropospheric ozone

https://doi.org/10.5194/egusphere-2025-2628
Preprint. Discussion started: 26 June 2025

variations governed by changes in stratospheric circulation. Nature Geoscience, 7, 340–344. https://doi.org/10.1038/ngeo2138, 2014.

Nieto, R., Gimeno, L., de la Torre, L., Ribera, P., Gallego, D., García-Herrera, R., García, J.A., Nuñez, M., Redaño, A., and Lorente, J.: Climatological Features of Cutoff Low Systems in the Northern Hemisphere. Journal of Climate, 18, 3085–3103. https://doi.org/10.1175/JCLI3386.1, 2005.

Ning, G., Yim, S. H. L., Wang, S., Duan, B., Nie, C., Yang, X., Wang, J., and Shang, K.: Synergistic effects of synoptic weather patterns and topography on air quality: a case of the Sichuan Basin of China. Climate Dynamics, 53, 6729–6744. https://doi.org/10.1007/s00382-019-04954-3, 2019.

Pierce, B., and Holloway, T.: When Stratospheric Ozone Hits Ground-level Regulation: Exceptional Events in Wyoming. Bulletin of the American Meteorological Society, 98, 889–892. https://doi.org/10.1175/BAMS-D-14-00133.1, 2017.

Prather, M. J., Zhu, X., Tang, Q., Hsu, J., and Neu, J. L.: An atmospheric chemist in search of the tropopause. Journal of Geophysical Research, 116, D04306. https://doi.org/10.1029/2010JD014939, 2011.

Shu, Z., Liu, Y., Zhao, T., Xia, J., Wang, C., Cao, L., Wang, H., Zhang, L., Zheng, Y., Shen, L., Luo, L., and Li, Y.: Elevated 3D structures of $PM_{2.5}$ and impact of complex terrain-forcing circulations on heavy haze pollution over Sichuan Basin, China. Atmospheric Chemistry and Physics, 21, 9253–9268. https://doi.org/10.5194/acp-21-9253-2021, 2021.

Shu, Z., Zhao, T., Chen, Y., Liu, Y., Yang, F., Jiang, Y., He, G., Yang, Q., and Zhang, Y.: Terrain effect on atmospheric process in seasonal ozone variation over the Sichuan Basin, Southwest China. Environmental Pollution, 338, 122622. https://doi.org/10.1016/j.envpol.2023.122622, 2023.

Shu, Z., Zhao, T., Liu, Y., Zhang, L., Ma, X., Kuang, X., Li, Y., Huo, Z., Ding, Q., Sun, X., and Shen, L.: Impact of deep basin terrain on $PM_{2.5}$ distribution and its seasonality over the Sichuan Basin, Southwest China. Environmental Pollution, 300, 118944. https://doi.org/10.1016/j.envpol.2022.118944, 2022.

Škerlak, B., Pfahl, S., Sprenger, M., and Wernli, H.: A numerical process study on the rapid transport of stratospheric air down to the surface over western North America and the Tibetan Plateau. Atmospheric Chemistry and Physics, 19, 6535–6549. https://doi.org/10.5194/acp-19-6535-2019, 2019.

Škerlak, B., Sprenger, M., Pfahl, S., Tyrlis, E., and Wernli, H.: Tropopause folds in ERA-Interim: Global climatology and relation to extreme weather events. Journal of Geophysical Research: Atmospheres, 120, 4860–4877. https://doi.org/10.1002/2014JD022787, 2015.

Škerlak, B., Sprenger, M., and Wernli, H.: A global climatology of stratosphere–troposphere exchange using the ERA-Interim data set from 1979 to 2011. Atmospheric Chemistry and Physics, 14, 913–937. https://doi.org/10.5194/acp-14-913-2014, 2014.

Sprenger, M., Maspoli, M. C., and Wernli, H.: Tropopause folds and cross-tropopause exchange: A global investigation based upon ECMWF analyses for the time period March 2000 to February 2001. Journal of Geophysical Research, 108, 8518. https://doi.org/10.1029/2002JD002587, 2003.

Stohl, A., Wernli, H., James, P., Bourqui, M., Forster, C., Liniger, M. A., Seibert, P., and Sprenger, M.: A New Perspective of Stratosphere–Troposphere Exchange. Bulletin of the American Meteorological Society, 84, 1565–1574. https://doi.org/10.1175/BAMS-84-11-1565, 2003.

Trickl, T., Bartsch-Ritter, N., Eisele, H., and Furger, M.: High-ozone layers in the middle and upper troposphere above Central Europe: potential import from the stratosphere along the subtropical jet stream. Atmospheric Chemistry and Physics, 11, 9343–9366. https://doi.org/10.5194/acp-11-9343-2011, 2011.

Trickl, T., Vogelmann, H., Giehl, H., Scheel, H.-E., Sprenger, M., and Stohl, A.: How stratospheric are deep stratospheric intrusions? Atmospheric Chemistry and Physics, 14, 9941–9961.

https://doi.org/10.5194/egusphere-2025-2628
Preprint. Discussion started: 26 June 2025

https://doi.org/10.5194/acp-14-9941-2014, 2014.
Venkat Ratnam, M., Ravindra Babu, S., Das, S. S., Basha, G., Krishnamurthy, B. V., and Venkateswararao, B.: Effect of tropical cyclones on the stratosphere–troposphere exchange observed using satellite observations over the north Indian Ocean. Atmospheric Chemistry and Physics, 16, 8581–8591. https://doi.org/10.5194/acp-16-8581-2016, 2016.
Wang, H., Wang, W., Huang, X., and Ding, A.: Impacts of stratosphere-to-troposphere-transport on summertime surface ozone over eastern China. Science Bulletin, 65, 276–279. https://doi.org/10.1016/j.scib.2019.11.017, 2020.
Wang, L., Li, M., Wang, Q., Li, Y., Xin, J., Tang, X., Du, W., Song, T., Li, T., Sun, Y., Gao, W., Hu, B., and Wang, Y.: Air stagnation in China: Spatiotemporal variability and differing impact on $PM_{2.5}$ and O_3 during 2013–2018. Science of the Total Environment, 819, 152778. https://doi.org/10.1016/j.scitotenv.2021.152778, 2022.
Wang, N., Du, Y., Chen, D., Meng, H., Chen, X., Zhou, L., Shi, G., Zhan, Y., Feng, M., Li, W., Chen, M., Li, Z., and Yang, F.: Spatial disparities of ozone pollution in the Sichuan Basin spurred by extreme, hot weather. Atmospheric Chemistry and Physics, 24, 3029–3042. https://doi.org/10.5194/acp-24-3029-2024, 2023.
Waugh, D. W., and Polvani, L. M.: Climatology of intrusions into the tropical upper troposphere. Geophysical Research Letters, 27, 3857–3860. https://doi.org/10.1029/2000GL012250, 2000.
Wei, J., Li, Z., Li, K., Dickerson, R. R., Pinker, R. T., Wang, J., Liu, X., Sun, L., Xue, W., and Cribb, M.: Full-coverage mapping and spatiotemporal variations of ground-level ozone (O_3) pollution from 2013 to 2020 across China. Remote Sensing of Environment, 270, 112775. https://doi.org/10.1016/j.rse.2021.112775, 2022.
Williams, R. S., Hegglin, M. I., Kerridge, B. J., Jöckel, P., Latter, B .G., and Plummer, D. A.: Characterising the seasonal and geographical variability in tropospheric ozone, stratospheric influence and recent changes. Atmospheric Chemistry and Physics, 19, 3589–3620. https://doi.org/10.5194/acp-19-3589-2019, 2019.
Xian, Y., Zhang, Y., Liu, Z., Wang, H., Wang, J., and Tang, C.: Source apportionment and formation of warm season ozone pollution in Chengdu based on CMAQ-ISAM. Urban Climate, 56, 102017. https://doi.org/10.1016/j.uclim.2024.102017, 2024.
Xu, X., Zhao, T., Liu, F., Gong, S., Kristovich, D., Lu, C., Guo, Y., Cheng, X., Wang, Y., and Ding, G.: Climate modulation of the Tibetan Plateau on haze in China. Atmospheric Chemistry and Physics, 16, 1365–1375. https://doi.org/10.5194/acp-16-1365-2016, 2016.
Yang, J., Wang, K., Lin, M., Yin, X., and Kang, S.: Not biomass burning but stratospheric intrusion dominating tropospheric ozone over the Tibetan Plateau. Proceedings of the National Academy of Sciences, 119, e2211002119. https://doi.org/10.1073/pnas.2211002119, 2022.
Yin, X., Kang, S., de Foy, B., Cong, Z., Luo, J., Zhang, L., Ma, Y., Zhang, G., Rupakheti, D., and Zhang, Q.: Surface ozone at Nam Co in the inland Tibetan Plateau: variation, synthesis comparison and regional representativeness. Atmospheric Chemistry and Physics, 17, 11293–11311. https://doi.org/10.5194/acp-17-11293-2017, 2017.
Yin, X., Rupakheti, D., Zhang, G., Luo, J., Kang, S., de Foy, B., Yang, J., Ji, Z., Cong, Z., Rupakheti, M., Li, P., Hu, Y., and Zhang, Q.: Surface ozone over the Tibetan Plateau controlled by stratospheric intrusion. Atmospheric Chemistry and Physics, 23, 10137–10143. https://doi.org/10.5194/acp-23-10137-2023, 2023.
Zhang, L., Guo, X., Zhao, T., Gong, S., Xu, X., Li, Y., Luo, L., Gui, K., Wang, H., Zheng, Y., and Yin,

https://doi.org/10.5194/egusphere-2025-2628
Preprint. Discussion started: 26 June 2025

X.: A modelling study of the terrain effects on haze pollution in the Sichuan Basin. Atmospheric Environment, 196, 77–85. https://doi.org/10.1016/j.atmosenv.2018.10.007, 2019.

Zhang, M., Tian, W., Chen, L., and Lü, D.: Cross-tropopause mass exchange associated with a tropopause fold event over the northeastern Tibetan Plateau. Advances in Atmospheric Sciences 27, 1344–1360. https://doi.org/10.1007/s00376-010-9129-9, 2010.

Zhang, Y., Li, J., Yang, W., Du, H., Tang, X., Ye, Q., Wang, Z., Sun, Y., Pan, X., Zhu, L., and Wang, Z.: Influences of stratospheric intrusions to high summer surface ozone over a heavily industrialized region in northern China. Environmental Research Letters, 17, 094023. https://doi.org/10.1088/1748-9326/ac8b24, 2022.

Zhao, K., Huang, J., Wu, Y., Yuan, Z., Wang, Yongwei, Li, Y., Ma, X., Liu, X., Ma, W., Wang, Ying, and Zhang, X.: Impact of Stratospheric Intrusions on Ozone Enhancement in the Lower Troposphere and Implication to Air Quality in Hong Kong and Other South China Regions. Journal of Geophysical Research: Atmospheres, 126, e2020JD033955. https://doi.org/10.1029/2020JD033955, 2021.